Fluidized Bed Spray Granulation – From process understanding to modeling of nucleation and dust integration
Proceedings of European Congress of Chemical Engineering (ECCE-6)
Copenhagen, 16-20 September 2007

Fluidized Bed Spray Granulation – From process understanding to modeling of nucleation and dust integration

G. Grünewald,[a] A. Dinkova,[a] M. Kind[a]

[a]*Institute of Thermal Process Engineering, University of Karlsruhe , D-76131 Karlsruhe, Germany*

1. Abstract

Fluidized bed spray granulation is a process to obtain coarse-grained particles directly from suspensions, solutions or melts, ready for sale without any need for post-treatment. The process combines spray drying with granulation and classification, thus allowing the product particle size distribution to be adjusted according to customer demands. Well-known applications include pharmaceutical products as well as mass products like detergents or fertilizer. Because of the process intensification combining several normally consecutive unit operations in one apparatus, it is imaginable, that design and specification of process parameters is mainly decided on the basis of intuition or experience, if available.

This is partly due to a lack of knowledge concerning the occurring mechanisms, but also due to the complex interaction of these mechanisms which makes it difficult to pre-estimate process behavior without simulation tools.

There are models published in literature helping to understand the process but still neglecting kinetics so far unknown like e.g. nucleation and dust integration. Both are important for a continuously running process deciding on whether it is possible to achieve steady state or not. In this work these mechanisms have been examined experimentally with the help of tracer methods in the case of dust integration and by analysis of continuous experiments in the case of nucleation (cf. (Grünewald et al., 2006)). On the basis of the findings, the kinetics of dust integration and seed formation have been modeled by combining strongly simplified fluid dynamics with deposition models and heat and mass transfer. The kinetics along with a population balance approach allows the dynamic modeling of the process including transient effects. The dust integration mechanism mainly controls the dust content in the plant and thus influences strongly the seed formation rate. The long-term experiments show a damped oscillating behavior of the particle size distribution and the production rate until achieving steady-state. The simulation results are able to reflect this behavior.

Keywords: fluidized bed spray granulation, nucleation, growth rate, tracer, dust integration

2. Introduction

In order to pre-estimate process behavior and decide on the parameter window for optimal operating conditions resulting in a stable steady-state process, it is necessary to be aware of the kinetics of the individual mechanisms occurring. It is even better to have quantitative knowledge and to be able to calculate the rates of the mechanisms. This makes it possible to run computer experiments prior to expensive laboratory validation when debugging running processes or establishing new products. When focusing on the granulation process, the model which is normally used for simulation is described in detail in (Heinrich and Mörl, 2002). The model is able to describe the dynamic behavior of the process, e.g. oscillations of the particle size distribution or the production rate. Thereby, the focus of the applications of the model was the investigation of a process layout with an external classification loop and milling of oversized product. In this model particle growth rate and attrition rate are assumed to be independent of particle size. Internal nuclei formation and dust integration are simply expressed by constant coefficients representing fractions of the dust available in the system being used for the mechanisms. Although all the kinetics rely on several simplifications or have to be adjusted with empirical constant coefficients, the model allows studying the dynamic behavior of the process and therefore helps to understand and visualize the complex interaction of the different mechanisms. The model was implemented in a commercial simulation package as shown by (Ihlow et al., 2004). A study of the stability of the process in dependence of different parameters like milling intensity, which means size and number of external nuclei, feed rate or fraction of dust used for nuclei production is presented by (Radichkov et al., 2006). They show numerically that parameters have to be within a certain range in order to result in a stable process instead of oscillating behavior. Thus, an operating window for an optimal process operation could be identified if the model was quantitative which is a limitation indicated by the author.

As already mentioned, in this model, rates are simplified particularly with respect to particle size independent behavior or simply just estimated by using a constant rate. Therefore the model is not able to describe internal nuclei production or dust integration. The dust content in the system is influenced by production because of attrition and overspray and consumption because of dust integration and seed formation. The instantaneous amount can not be balanced properly without the knowledge of the mechanisms and their kinetics. This work tries to diminish this lack of knowledge and shows experimental methods as well as theoretical approaches to deal with this problem. It will provide an overview of all the different approaches instead of detailed results and dependencies, which will be discussed in detail separately.

Considering continuously operated granulation, four mechanisms are important, namely droplet deposition on particles, dust formation, dust integration into wet particles and nucleation. Depending on the material system and the operating parameters, agglomeration between larger granules and breakage also play a role but were excluded in this case. Following the compartment model approach of (Becher, 1997), (Zank et al., 2001a) examined drop deposition and modeled the kinetics by

considering particularly the nozzle region of a submerged jet in a shallow fluidized bed. The model reminds of a simplified Lagrangian approach, considering particle group behavior. Consequently particle size dependent drop deposition and therefore particle size dependent growth rates can be calculated. Furthermore dust production as a result of overspray and splashing of impinging drops can be obtained by this model.

In this work dust integration and nucleation were investigated experimentally and described theoretically. In order to deduce the kinetics of dust integration, semi-batch experiments were carried out where tracer-marked dust was supplied at the beginning. Thus, by analyzing the particles with respect to tracer content after the experiment, the amount of dust incorporated into growing particles could be calculated. In order to verify the dust contribution to growth in continuous operation, steady state experiments were conducted with constant mass flow rates of dust supplied into the nozzle region.

The kinetics of nucleation was investigated by steady-state experiments obtaining the effective nucleation rate directly as the difference of the number streams of particles entering and leaving the apparatus.

On the basis of the experimental findings the kinetic model of Zank was extended to describe nucleation and dust integration. In order to allow dynamic calculations, the kinetic model was combined with the population balance discretization as described in (Kumar et al., 2006).

3. Experimental investigations

3.1. Experimental set-up

The experimental set-up is shown in Fig. 1. The fluidized bed with a diameter of 230 mm is equipped with a perforated air distributor. A lateral channel blower aspirates ambient air flowing through an electrical heater before entering the fluidized bed. The fluidization air leaves the apparatus through an outlet at the top. The elutriated fine particles are collected in an external filter with 4 filter bags. The dust is returned into the fluidized bed through a pipe passing a sluice system and a switch point which allows the sampling or removing of the dust from the system. A two-fluid nozzle is positioned centric at the bottom spraying upwards through the bed of particles. The air jet sweeps along granules from the fluidized bed, thus causing a circulation of the particles through the nozzle region.

A constant particle stream, limited by a cellular wheel sluice leaves the apparatus towards an external air classifier (zig-zag air separator). A switch in the pipe allows the automated sampling and feeding of the samples directly into an optical particle size distribution measurement device. Particles with product size passing the classifier are collected on a balance, smaller particles are pneumatically returned into the granulation chamber at about 1 m above the fluidized bed. If external nuclei are supplied, they are fed into this backflow pipe by a gravimetric dosing system. In order to limit the bed height to an upper value, it is possible to discharge particles by an overflow pipe.
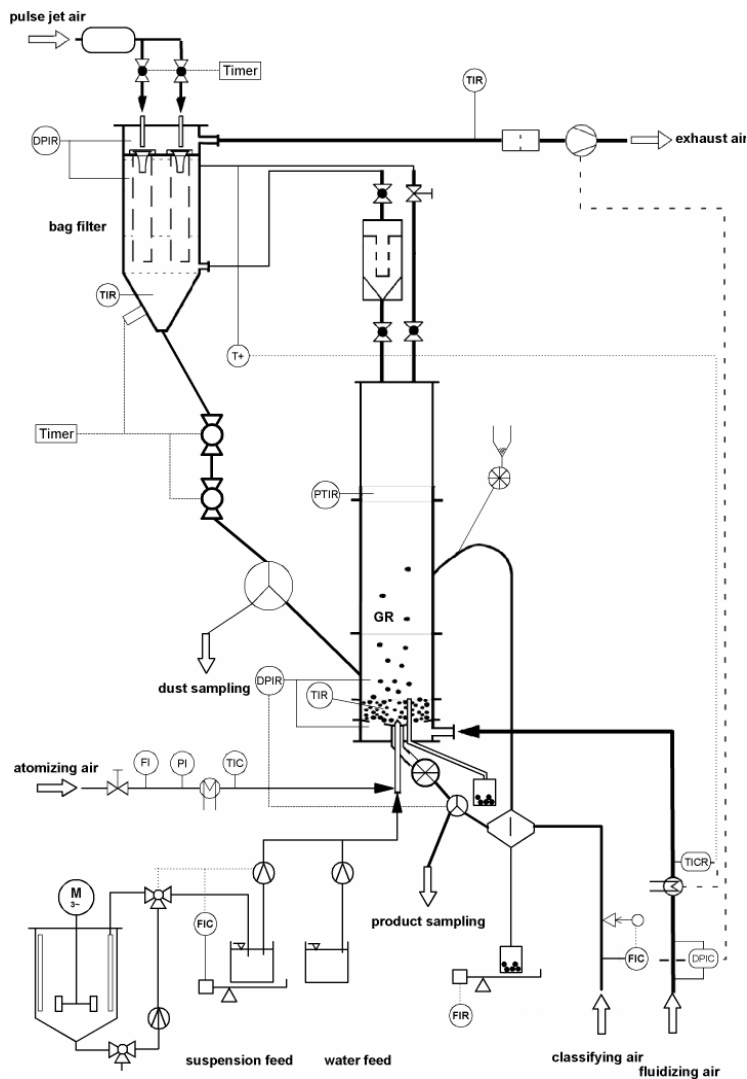
Fig. 1: Experimental set-up

3.1.1. Materials and instruments

The fluidization air is heated ambient air, whereas the atomizing air of the two-fluid nozzle and the air for the classifier are compressed air. Feed liquid is a suspension of limestone (Calcilit 4G, Alpha Calcit Füllstoff GmbH, Germany, particle sizes 0-10µm, $d_{3,0} = 3µm$). Polyvinylpyrrolidon (Kollidon 30, BASF AG, Germany) is used as binder material.

The particle size distributions of granules were measured by optical image analysis (Camsizer 2006, Retsch Technology GmbH, Germany), the dust size distributions were measured with laser diffraction analysis (Mastersizer S, Malvern Instruments Ltd, England). The tracer analyses were done with Inductively Coupled Plasma Optical Emission Spectroscopy (VistaPro CCD Simultaneous ICP-OES, Varian Inc., USA).

3.1.2. Standard operating conditions

Unless otherwise noted, the operating conditions indicated in Table 1 were used for all experiments where applicable (e.g. batch experiments do not have an external nuclei supply).

Table 1: Standard operating parameters for all experiments (where applicable)

$u_0 \left[\frac{m}{s}\right]$	0.7	$\dot{M}_F \left[\frac{kg}{h}\right]$	4.3	$d_{3,0,nuclei} [\mu m]$	285
$\vartheta_{fl} [°C]$	150	$x_s \left[\frac{kg}{kg}\right]$	0.35	$\dot{M}_{nuclei} \left[\frac{kg}{h}\right]$	0.1
$\dot{M}_{G,n} \left[\frac{kg}{h}\right]$	12	$x_{PVP} \left[\frac{kg}{kg}\right]$	0.06	$t_{filter} [s]$	30
$\vartheta_{G,n} [°C]$	30			$d_{sep} [\mu m]$	106
$\vartheta_{G,out} [°C]$	60°C			$M_{0,dust} [kg]$	1

If dust was recycled into the granulation chamber, standard recycling location was through a pipe welded on the side of the granulation chamber down through a channel into the fluidized bed.

3.1.3. Semi-batch experiments with tracer-marked dust to investigate dust integration

In order to distinguish between growth of particles by drop deposition and by dust integration, semi-batch experiments were carried out with tracer-marked dust. At the beginning of the experiment, a bimodal particle distribution (300-400µm and 500-750µm, 300g each) and 1kg of tracer-marked dust were supplied. The dust was produced in the same apparatus used as a spray dryer with 2.5 mass-% of KNO3 added to the suspension. In regular intervals during the experiment, particle samples were taken and after classification, acid pulping and appropriate preparation, the concentration of potassium was measured with Inductively Coupled Plasma Optical Emission Spectroscopy (OCP-OES). ICP-OES is a standard method for trace analysis in water chemistry and is able to measure concentrations in the range of ppm if properly calibrated. Since the concentration of tracer in the supplied dust is known, it is possible to deduce dust integration quantity from measured concentration values.

3.1.4. Steady-state experiments to measure nucleation rates and dust integration

The formation rate of seed particles in the dust is difficult to measure quantitatively since measurement devices based on laser diffraction are the only possibility to get the particle size distribution in this size range. These devices do not count particles of particular size classes but determine a best fit of the whole distribution. The acquired information about the number of seed particles is not reliable, since the high numbers of smaller dust particles dominate the distribution. The solution is the detection of the number streams entering and leaving the apparatus in steady-state operation. Then, the internal nucleation rate can easily be calculated as the difference of all other known streams:

$$\dot{N}_{nuclei,int} = \frac{\dot{M}_{overflow}}{\rho_p \cdot \frac{\pi}{6} \cdot d_{3,0;overflow}^3} + \frac{\dot{M}_{product}}{\rho_p \cdot \frac{\pi}{6} \cdot d_{3,0;product}^3} - \frac{\dot{M}_{nuclei,ext}}{\rho_p \cdot \frac{\pi}{6} \cdot d_{3,0;nuclei,ext}^3} \qquad (1)$$

To start the experiment, the apparatus and the starting material (hold-up of dust and particles of the preceding steady-state experiment) was heated to operating

temperature. Then, suspension feed, external nuclei feed, dust recycling and classifying particle outlet were started. Achievement of steady-state operation was detected by constant temperatures, particle size distribution, product stream and pressure drop of the fluidized bed for about 1-2 residence times in the granulator (eq. (2)).

$$\tau = \frac{M_{fb}}{\dot{M}_F \cdot x_s + \dot{M}_{nuclei,ext}} \qquad (2)$$

Then feed was switched from suspension to water, inlet and outlet streams were stopped and dust as well as granules was discharged from the system. Normally, time to achieve steady-state takes from 8-12 hours.

Steady-state experiments were also carried out to determine the influence of dust integration on particle growth rate. For these investigations, a constant dust mass flow (6 kg/h) was supplied at different heights (0, 15, 45 mm) above the nozzle into the spray jet. Because of steady-state conditions, the integration of the steady-state population balance can be used to determine the particle growth rate (cf. (Zank et al., 2001b)):

$$G(d) = \frac{\dot{N}_{nuclei,ext} \cdot Q_{0,nuclei,ext}(d) - \dot{N}_{overflow} \cdot Q_{0,overflow}(d) - \dot{N}_{product} \cdot Q_{0,product}(d)}{N_{fb} \cdot q_{0,fb}(d)} \qquad (3)$$
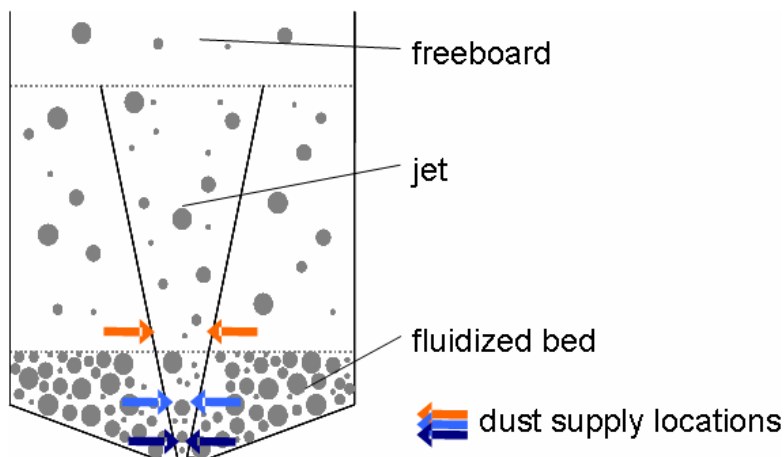
Fig. 2: Dust supply locations into the spray jet (0, 45 mm depicted)

3.1.5. *Velocity measurements to validate fluid dynamics calculations*

The fluid dynamics in the fluidized bed, especially in the jet region, plays an important role for the mechanisms of drop deposition, dust integration and seed formation. In the compartment model to dynamically simulate experiments, a simplified semi-empirical fluid dynamics calculation was implemented (cf. Becher, Zank). In order to verify the model beyond the measurements of (Zank, 2003), computational fluid dynamics (Fluent, Ansys, Inc.) was used to get local information in the jet region.

Experimental validation of local particle and drop velocities in the jet above the shallow fluidized bed was done with Laser Doppler Anemometry and Particle Image Velocimetry (see Fig. 3). In order to measure these velocities, there is a larger cutout and two smaller cutouts perpendicular to the first one in the granulation chamber,

covered air tight with glass windows. Thus, optical access with laser and CCD-camera is possible which allows contactless measurements.

Laser Doppler Anemometry can be used without any calibration and is very accurate in a wide range of particle sizes and velocities. A disadvantage of this system is the pointwise acquirement of values with only one velocity component. Particle Image Velocimetry covers the whole observation area, but is very sensitive to the quality of the CCD-pictures. It needs to be calibrated and accuracy decreases with increasing size of tracer particles and decreasing number concentrations.
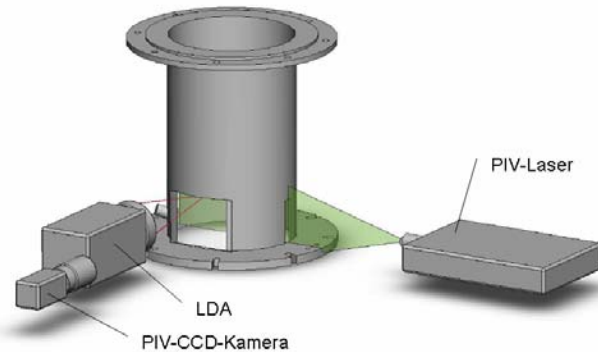
Fig. 3: Set-up with LDA- and PIV-system for contactless velocity-measurements inside the granulation chamber

4. Modeling of the kinetics

The process model is designed as a compartment model. Fig. 4 visualizes the division and the interconnections of the individual zones by material streams. Each phase in each zone has its own set of equations describing mass and energy conservations.

The jet has to be described in more detail compared to the other compartments, since fluid dynamics plays a role in the description of the mechanisms. Propagation velocity of the jet is very high because of the high gas velocity at the nozzle orifice. Thus, a quasi-stationary description is appropriate and the equations have to be set up in terms of local rather than temporal changes. Because of the periodic filter dedusting, boundary conditions of the jet change continuously. This requires a frequent calculation of the jet throughout the simulation run. The jet calculations provide the rates for the growth of particles and the seed formation needed in the temporal modeling of the process. Because of the frequent calculations, simulation time is about 10 times longer than process time.

The kinetics of dust integration and nucleation is crucial for the whole process. Therefore we will focus here on the jet calculations where the kinetics is obtained from.

Fig. 4: Assembly of the compartment model with streams of the different phases

The most important assumptions are:
- Particles are sucked into the jet with their particle size distribution in the fluidized bed.
- All particles in one size class behave the same, which means e.g. moisture of a particle is total moisture of a size class divided by particle number in this class.
- Dust and seed particles are treated as air loading just like moisture and follow the air fluid dynamics.
- Dust, that takes part in the mechanisms of seed formation and dust integration has only one particle size (mean measured particle size $d_{3,0} \approx 3\mu m$).
- Seed particles are treated like granules in terms of particle growth.
- The energy balance for the dust loop to and from the filter is not considered

Fig. 5 shows an axis-symmetric control element in the jet with all the phases entering and leaving and the schematic depiction of the mechanisms.

Fig. 5: 2D-axis-ymmetric control volume in the jet region with mass flows and their loadings as well as mechanisms (schematic)

- Seed formation is calculated as a rate along the jet propagation. One seed particle is considered to be the agglomerated product of one drop with dust particles. In order to obtain the number of seed particles, which are formed in a control volume, the deposition of dust particles on drops is calculated. The number of seed particles is the total deposited mass of dust divided by the mass necessary to form one seed particle. Therefore a seed particle size has to be assumed. The deposition efficiency is an arbitrary parameter, since dust particles and drops both are small enough to follow the airflow. Furthermore effects like non-uniform distribution of the different phases in the spray can not be described. After the integration of the jet, the current seed formation rate can be obtained.

$$\frac{dc_{dust}}{dz} = -\eta_{dust} \cdot \frac{3}{2} \cdot \frac{1-\varepsilon_{drop}}{\varepsilon_P} \cdot \frac{c_{dust}}{d_{drop}} \qquad (4)$$

$$d\dot{N}_{dust} = d\left(c_{dust} \cdot \dot{V}_G\right) \qquad (5)$$

$$d\dot{N}_{seed} = -d\dot{N}_{dust} \cdot \frac{m_{dust}}{m_{seed} - x_{s,drop}(z) \cdot m_{drop}(z)} \qquad (6)$$

- Particle movement is described with coupled momentum balances for air and each particle class. Thus, the local velocities of the different particle sizes along the axis in the jet are obtained. Momentum is averaged over each particle class. In a separate model, different entry positions of particles in the jet were considered as additional dimension. This caused a tremendous increase in calculation time, but the differences of the growth rates were marginal.

$$\frac{d\left(\dot{M}_{P+seed,z} \cdot u_{P+seed,z}\right)_i}{dz} = \frac{d(\dot{M}_{P,rad} \cdot u_{P,rad,z})}{dz} + \frac{dF_{d,i}}{dz} + \frac{dF_{b,i}}{dz} - \frac{dF_{gr,i}}{dz} \qquad (7)$$

$$\frac{d\left(\dot{M}_{G,z} \cdot u_{G,z}\right)_i}{dz} = \frac{d(\dot{M}_{G,rad} \cdot u_{G,rad,z})}{dz} + \frac{dF_b}{dz} - \frac{dF_{gr}}{dz} - \sum_i \frac{dF_{d,i}}{dz} - \frac{dF_{shear}}{dz} \qquad (8)$$

To solve equation (8), the shear force is assumed to be responsible for the gas entrainment into the jet. The other forces are responsible for the velocity change of the gas. The turbulent shear force is calculated according to Prandtl's mixture length approach. Both momentum equations (gas and particles) are coupled by the drag force of the particles ($F_{d,i}$).

- The drying kinetics is described by the heat and mass transfer models of spheres in a surrounding air flow ((VDI-Wärmeatlas, 2002)). The falling-rate drying period was taken

into account by the dimensionless drying curve obtained by gravimetric experiments in an air channel. The moisture of each particle class is increased by drop deposition and decreased by drying. In order to get the effective wet surface of the particles taking part in mass transfer, an assumption of the film height is necessary. Therefore experiments with a high-speed camera were carried out to get an idea for the ratio of film height to drop diameter. It was found that 40% of the initial drop diameter is a good guess for the effective film height.

- Drop and dust deposition on particles is modeled with the wet scrubber model which can be found in (Löffler, 1988). The deposition rate is made up of impingement efficiency and adhesion efficiency (eq. 11). Inertial deposition is considered to be the dominating mechanism (eq. 9). Adhesion efficiency of drops is described following the experimental findings of (Mundo et al., 1995) defining a critical impact velocity depending on the dimensionless Oh-number, (eq. 10). Adhesion efficiency of dust is considered to be directly proportional to the fraction of wet surface of the granules which is still not occupied by dust particles (eq. 12). In order to get local information about the unoccupied wet surface, it has to be balanced separately.

$$\varphi = \left(\frac{St}{St + a} \right)^b \tag{9}$$

$$h_{drop} = \left(\frac{u_{crit,\perp}}{u_{rel}} \right)^2 \tag{10}$$

$$\frac{d\dot{N}}{dz} = \eta \cdot \frac{\pi}{4} \cdot d_P^2 \cdot u_{rel} \cdot \frac{1}{\dot{V}_G} \cdot \dot{N}_{drop} \cdot \frac{dN_{P+seed}}{dz} \tag{11}$$

$$h_{dust} = \left(\frac{d_P^*}{d_P} \right)^2 \tag{12}$$

5. Results

5.1. Dust integration rate and its contribution to total particle growth rate

One goal of the experimental investigations was to distinguish between growth of particles by drop deposition and by dust integration. This could be realized by the semi-batch experiments with tracer-marked dust. Fig. 6 shows exemplarily the findings for the experimental runs with three different fluidization air temperatures. The samples were taken every 5 minutes showing the temporal trend of the dust integration. Since a bimodal particle size distribution was used, the individual behaviour of smaller and larger particles could be investigated. Dust tracer content was measured too, thus tracer dilution in the dust during the experiment is included in the results.
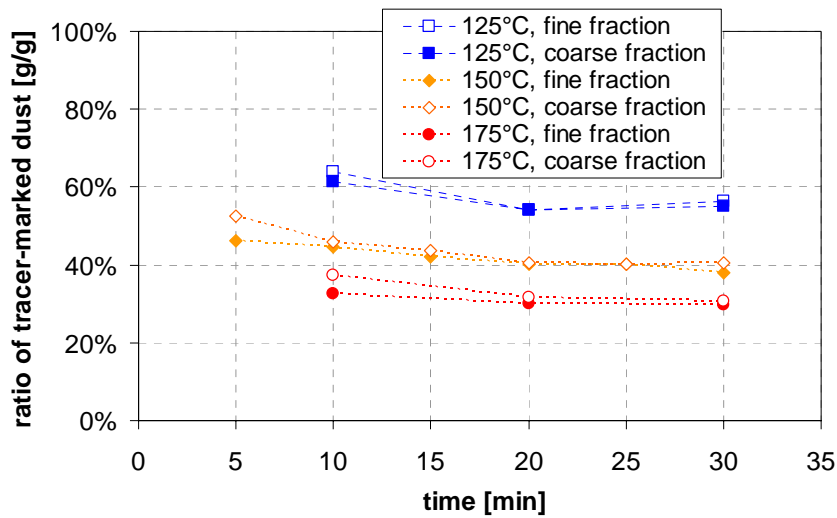
Fig. 6: Tracer, resp. dust content of different particle fractions for various fluidization air temperatures

As expected, lower temperatures cause a significant increase of dust integration. The drying rate of the particles decreases and their wet surface, which is responsible for dust integration, increases. In these experiments, a reduction of 50°C doubled the incorporation of tracer-marked dust into the growing particles. Dust integration slightly falls with time although tracer dilution was considered. This can be due to a reduction of the amount of dust in the system or due to the dust getting coarser because of agglomeration processes. Other experiments, which will not be discussed here, showed, that dust coarseness also had a significant influence on the dust integration rate. Unexpectedly the rate with which dust integration contributes to total particle growth is independent from particle size. This implies that dust integration is more or less proportional to drop deposition.

5.2. Nucleation rate

The nucleation rate was obtained in steady-state operation evaluating number streams and particle size distributions (cf. 3.1.3). Fig. 7 shows the total nuclei rate in dependence of a dimensionless factor, the ratio of dust to particle hold-up in steady-state operation. This ratio was used, since dust concentration and fewer particles in the granulator were found to increase nucleation rate. Thus increasing the ratio of these two parameters seems to exponentially enhance nucleation. The experimental series were carried out with different fluidization numbers as indicated. A lower fluidization number significantly increases nucleation rate at the same dust to particle ratio. This is due to an increase of the residence time of dust in the fluidized bed and thus an increase of the dust concentration in the spray. A high fluidization number almost eliminates any nucleation. The two horizontal lines between $2 \cdot 10^6$ and $5 \cdot 10^6$ indicate the range of the external nuclei rate for all the experiments.
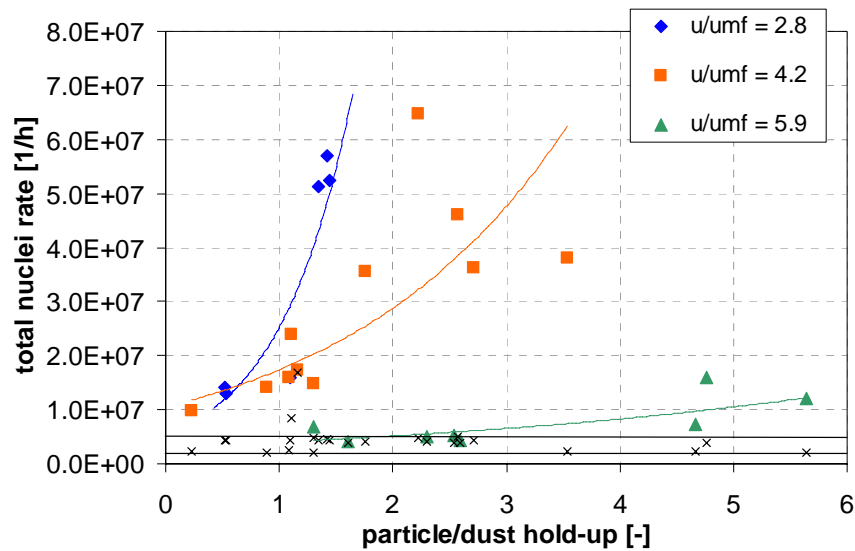
Fig. 7: Total nuclei rate in dependence of particle and dust hold-up, variation of fluidization rate
(horizontal lines mark the range of external nucleation rate)

The high concentrations of dust needed to achieve equilibrium of dust production and dust consumption, is reflected by the steady-state dust hold-up for different fluidization numbers in Fig. 8. A certain fluidization number results in a characteristic amount of dust necessary for an adequate dust integration. This supports the explanation given above basing on reduced dust residence time and thus reduced kinetics.
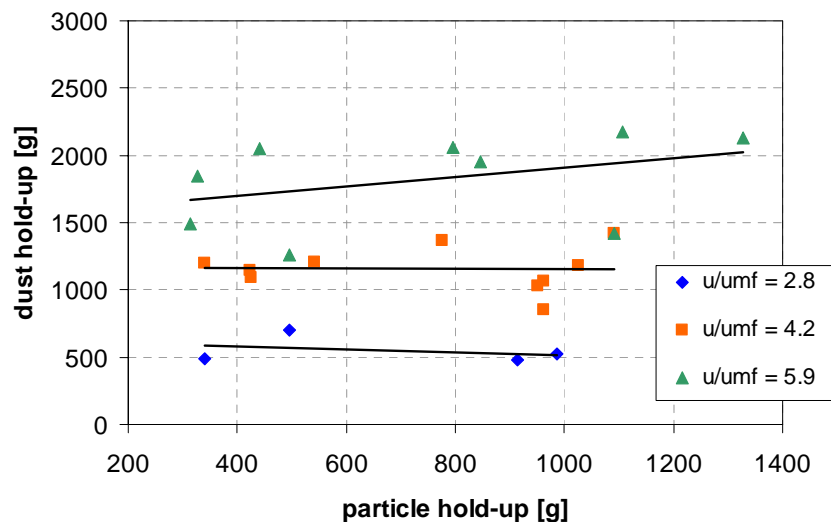
Fig. 8: Dust hold-up in dependence of particle hold-up in steady-state operation, variation of fluidization rate

5.3. Velocity measurements and CFD-calculations

Particle, drop and dust velocities in the jet, especially the relative velocities between the different phases, have a significant influence on the different mechanisms of deposition. Velocity measurements with Laser Doppler Anemometry and Particle Image Velocimetry were used to validate the kinetics model as well as CFD-

calculations. With the help of CFD, it is possible to get an idea of the whole flow field in the apparatus, not just the local information where optical access is possible. This allows further investigations, for example particle size dependent residence times in the upper part of the apparatus, determining particle moisture content when returning to the fluidized bed. This is necessary when taking agglomeration of the particles into account. Fig. 9 shows the vertical component of particle velocity in the jet 70 mm above the nozzle orifice. The particle velocity in the two-phase flow reminds of the profile of an open air jet. LDA and PIV values are very close together, although the big particles with their comparatively low number concentration are not ideal tracer particles for a PIV-system. This has to be kept in mind when running the analysis of the measured data. With increasing mass flow of atomizing air, maximum particle velocity increases linearly.
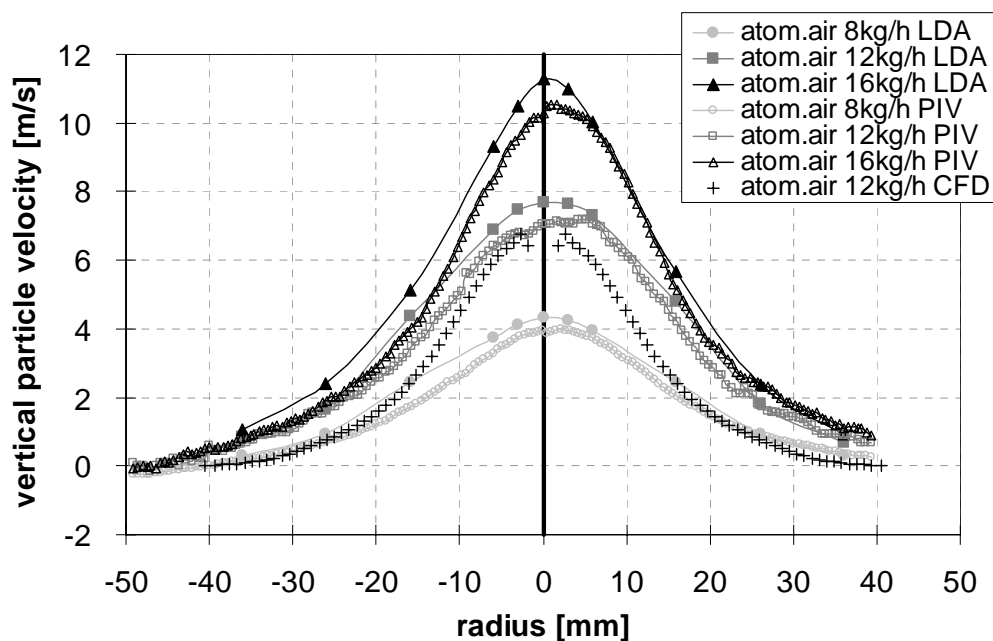
Fig. 9: Vertical particle velocity profile in the jet measured with LDA and PIV 70 mm above the nozzle orifice (Exemplarily: CFD-calculations for 12kg/h atomization air)

The CFD-calculations will not be discussed here. Fig. 9 just shows one example of calculated particle velocities in the jet at 70 mm above the nozzle orifice for 12kg/h atomization air.

Depending on the boundary conditions of the atomizing air inlet, there are slightly different profiles. Altogether, CFD is able to satisfyingly describe the two-phase flow of air and particles resulting from the submersed nozzle with the jet penetrating the fluidized bed. Especially the maximum velocities are close together, whereas jet width is underestimated by CFD.

The simulation of the fluid dynamics can be extended by user defined functions, which was done e.g. to calculate the drop deposition in the spray. Fig. 10 shows exemplarily the integral total drop deposition efficiency in the jet over jet height above the nozzle. It is obvious, that the drop deposition is completed after a length of about 80 mm, which agrees with the findings of for the simplified model.
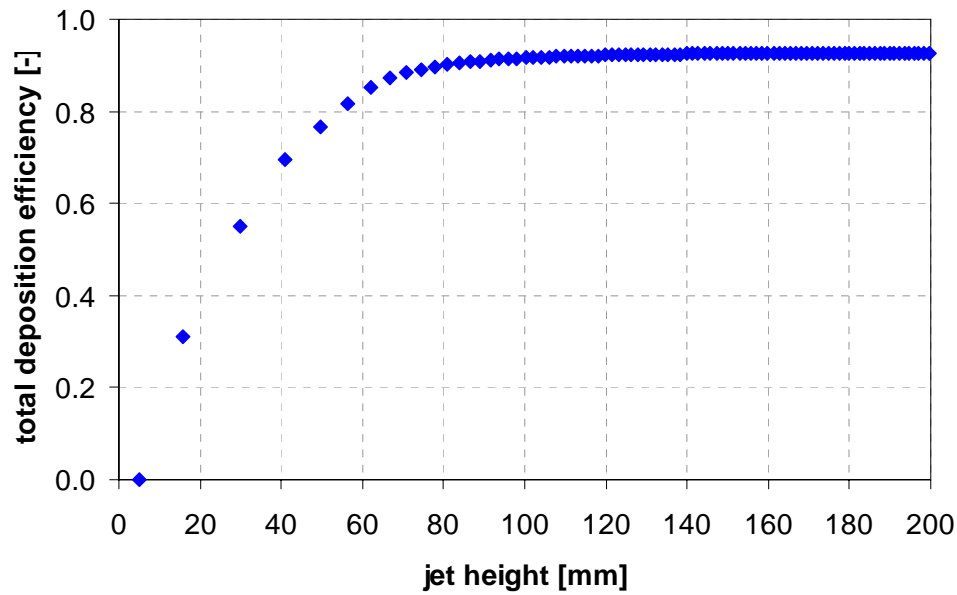
Fig. 10: Integral total deposition efficiency of drops over jet height above the nozzle

5.4. Results of the kinetic model

In order to predict process behavior with the help of a simulation tool, the different kinetics of the mechanisms has to be described satisfactorily. Fig. 11 shows the contribution of the dust integration to total particle growth obtained from the quasi-steady-state jet calculations. The fraction of dust integration is almost independent from particle size at a value of about 35%. This is close the experimental findings of the tracer investigations with 150°C as fluidization air temperature.
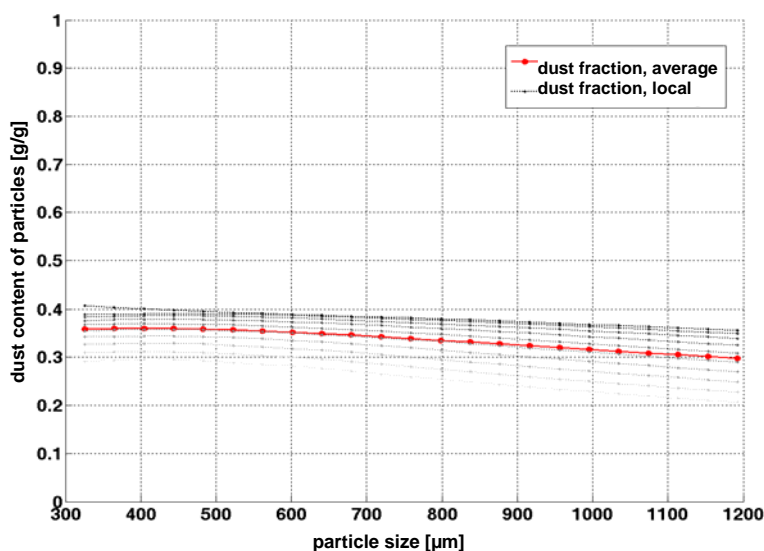
Fig. 11: Contribution of dust integration to total particle growth rate for different particle sizes

Fig. 12 displays the total particle growth rate for two dust entry locations in the jet as indicated in the small drawing. The measured values obtained from steady-state

experiments are compared to calculated growth rates for the same conditions. The model describes the coherences quite well, although the calculated values decline slightly too fast with decreasing particle size. This might underestimate the growth of small particles in long-term simulations.
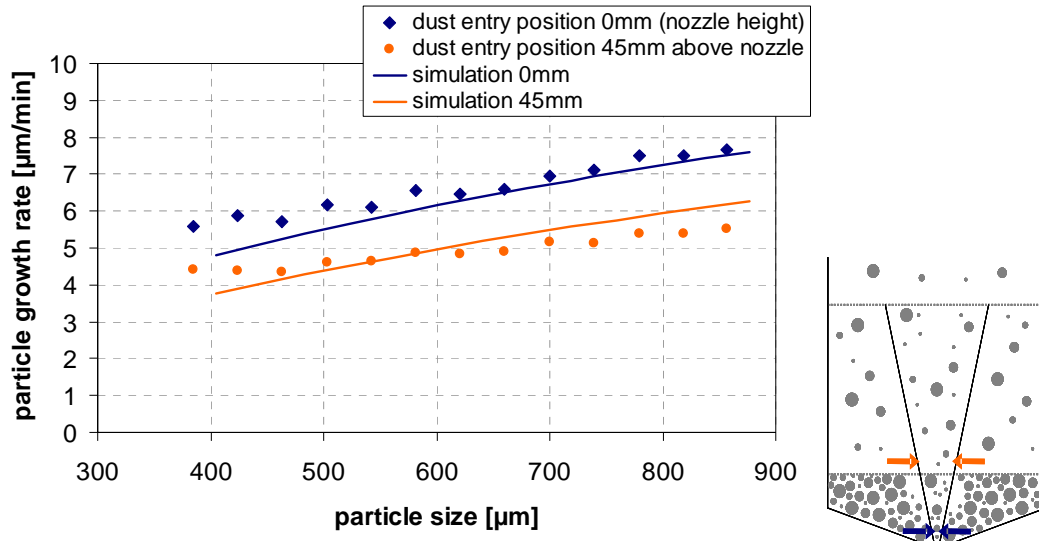
Fig. 12: Particle growth rate measured and calculated for different dust entry locations in the jet

The kinetics of dust integration is necessary for the correct balance of dust content in the system. The calculation of the nucleation rate allows the simulation of the evolution of the particle size distribution in the system. Fig. 13 shows first results of these simulations, which are done at the moment and will be reported soon. The first peak of the distribution stands for the internal nuclei which approach the second peak representing external nuclei supply.
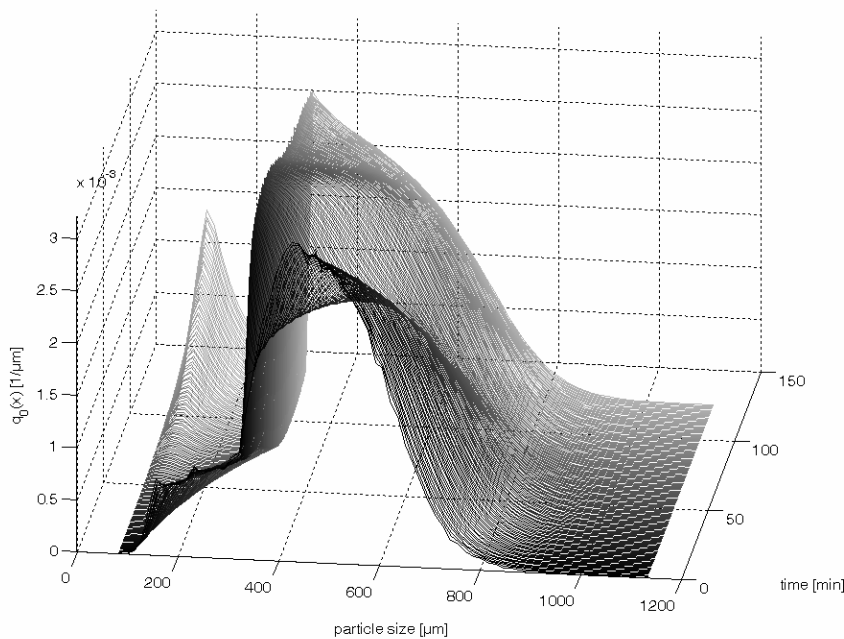
Fig. 13: Temporal evolution of particle size distribution with internal and external nucleation

6. Conclusions

This work demonstrates an overview of several methods for the investigation of the complex and connected mechanisms of the fluidized bed granulation process. Quantitative knowledge about the dust integration rate is necessary to balance dust content in the system and thus correctly calculate the internal nucleation rate. Dust integration is mainly dependent on particle moisture content, fluid dynamics as far as deposition mechanisms are concerned and total dust content in the system. An example was provided showing the significant increase of dust integration by growing particles with decreasing temperature in the system and thus decreased particle drying rate. From these findings and the fact that dust contribution to total particle growth is independent from particle size leads to the conclusion, that dust integration is proportional to drop deposition with dust concentration controlling the actual value.

Concerning the nucleation rate, there are two limitations. For the nucleation mechanism, dust particles have to meet droplets to agglomerate. Therefore, at a given location in the spray, droplets might already be deposited on particles, or dust concentration might be low, both hindering the agglomeration process. Thus, concentrations of both, droplets and dust particles, might limit the nucleation rate. Any other mechanism or boundary condition in the process, which reduces any of these populations, indirectly reduces the nucleation rate. One example was given by the fluidization number which reduces dust residence time in the fluidized bed and enhances entrainment to the filter. With increasing fluidization number, nucleation rate falls significantly. Furthermore, the dimensionless value representing dust to particle hold-up ratio has to be increased to enhance nucleation rate. This means, a lower fluidized bed or a higher dust concentration in the system promotes nucleation.

A model of the process has to describe all these mechanisms, which is demonstrated on the example of dust integration contributing to total particle size dependent growth rate. Dust concentration in the spray plays a role, which is shown by decreasing particle growth rate with increasing distance of dust supply location from the nozzle orifice. Furthermore an example case was shown to demonstrate internal nucleation rate, which has to be pursued further.

Notations

a, b	constant factors (deposition efficiency), -
c	concentration, $\#/m^3$
d	particle size, m
d^*	diameter of spherical segment, which is wet and unoccupied, m
$d_{3,0}$	representative particle diameter, m
dz	height of control volume, m
F	force, N
FB	freeboard
G	particle growth rate, m/s
h	adhesion efficiency, -
jet	jet-related

m	mass of one particle, kg
M	mass, kg
M_0	initial mass, kg
$\dot{M}$	mass flow rate, kg/s
$\dot{N}$	number stream, #/s
N	number, #
$\dot{Q}$	heat flux, W
q_0, Q_0	(cumulative) number distribution, 1/m
t	time, s
u	velocity, m/s
u_0	superficial velocity, m/s
$\dot{V}$	volume flow, m³/s
x	mass fraction, kg/kg
Y	loading of gas (water, dust), -
z	height above nozzle, m
ε	porosity, -
φ	impingement efficiency, -
η	deposition efficiency, -
ϑ	temperature, °C
ρ	density, kg/m³
τ	residence time, s

Dimensionless numbers

St	Stokes number, -

subscripts

$\perp$	at right angle
b	buoyancy
class	classifier
crit	critical
d	drag
drop	droplet, spray related
dust	dust
exhaust	exhaust
ext	external
F	feed
fb	fluidized bed
filter	filter
F	film
fl	fluidization air
G	gas
gr	gravitation
H_2O	water
i	particle size-class index

int	internal
mf	minimal fluidization
N	nozzle
nuclei	nuclei
out	outlet
overflow	overflow
product	product
P	particle
PVP	Polyvinylpyrrolidon
rad	radial
rel	relative
s	solid
seed	seed
sep	separation
shear	shear
susp	suspension

Acknowledgements

References

Becher, R.-D. (1997), *Untersuchung der Agglomeration von Partikeln bei der Wirbelschicht-Sprühgranulation*, PhD thesis, Universität Fridericiana Karlsruhe (TH)

Grünewald, G. et al. (2006), Experimental methods to investigate seed formation and dust integration in a fluidized bed spray granulation process, 15th International Drying Symposium, 816-821

Heinrich, S. and Mörl, L. (2002), Analysis of the start-up process in continuous fluidized bed spray granulation by population balance modelling, *Chemical Engineering Science*, 57, 4369-4390

Ihlow, M. et al. (2004), A new comprehensive model and simulation package for fluidized bed spray granulation processes, *Chemical Engineering & Technology*, 27, 1139-1143

Kumar, J. et al. (2006), Improved accuracy and convergence of discretized population balance for aggregation: The cell average technique, *Chemical Engineering Science*, 61, 3327-3342

Löffler, F. (1988), *Staubabscheiden*, Thieme, Stuttgart

Mundo, C. et al. (1995), Droplet-Wall Collisions: Experimental Studies of the Deformation and Breakup Process, *Int.J.Multiphase Flow*, 21, 151-173

Radichkov, R. et al. (2006), A numerical bifurcation analysis of continuous fluidized bed spray granulation with external product classification, *Chemical Engineering and Processing*, 45, 826-837

VDI-Wärmeatlas (2002), *Berechnungsblätter für den Wärmeübergang*, 9. Auflage, Springer-Verlag, Berlin Heidelberg

Zank, J. et al. (2001a), Particle growth and droplet deposition in fluidised bed granulation, *Powder Technology*, 120, 76-81

Zank, J. et al. (2001b), Particle growth in a continuously operated fluidized bed granulator, *Drying Technology*, 19, 1755-1772

Zank, J. (2003), *Tropfenabscheidung und Granulatwachstum bei der Wirbelschicht-Sprühgranulation*, PhD thesis, Universität Fridericiana Karlsruhe (TH)